

Probing the electronic effect of carbon nanotube in catalysis: NH₃ synthesis over Ru nanoparticles

Shujing Guo,^[a] Xiulian Pan,*^[a] Haili Gao,^[b] Zhiqiang Yang,^[a] Jijun Zhao,^[b] Xinhe Bao*^[a]

Abstract: Carbon nanotubes (CNTs) have been shown to modify some properties of nanomaterials and chemical reactions confined inside their channels, which are formed by curved graphene layers. Here we studied ammonia synthesis over Ru as a probe reaction in order to understand the effect of the electron structure of CNTs on the confined metal particles and their catalytic activity. The catalyst

with Ru nanoparticles dispersed almost exclusively on the exterior nanotube surface exhibits a higher activity than the CNT-confined Ru although both have a similar metal particle size. Characterizations with TEM, BET, chemisorption, temperature programmed reduction, CO adsorption microcalorimetry and first principles calculations suggest that the outside Ru exhibits a higher electron density

compared to the inside Ru. As a result, the dissociative adsorption of N₂, which is an electrophilic process and the rate-determining step of ammonia synthesis, is more facile over the outside Ru than that over the inside one.

Keywords: carbon nanotube • ruthenium • ammonia synthesis • CO adsorption microcalorimetry • first principles calculations

Introduction

Carbon nanotubes (CNTs) distinguish themselves from other carbon materials such as activated carbon and carbon nanofibers because they have a well-defined tubular structure formed by graphene layers. The diameter of these tubes typically ranges from less than 1 to 100 nm, which opens up opportunities to study chemistry in such confined environments. For example, fullerene and its derivatives, alkali metals and halides, transition metals and metal oxides have been introduced there and the resulting composites often exhibited properties differing from their parent materials.^[1-4] In addition, theoretical studies predicted that chemical reactions are sensitive to the confinement in these nanoscopic channels and their reaction rates can be modified due to interactions with the graphene walls of CNTs compared to those in the gas phase.^[5-6]

Our previous studies showed that the redox properties of metal and metal oxide nanoparticles were modified when they were confined inside the CNT channels.^[7] For example, the reduction of confined iron oxide was facilitated with respect to the outside iron oxide particles and it became more facile with decreasing CNT

channel diameter. On the other hand, the oxidation of metallic iron inside CNTs was retarded with respect to those dispersed on the exterior CNT surface. We proposed there that it was possibly the result of interactions between metal nanoparticles and CNT surfaces.^[7-8] Earlier theoretical studies have shown that CNTs exhibit a unique electron structure. In particular, the sp² hybridized orbitals of carbon are deformed due to the curvature of graphene walls, with π electron density shifting from the concave interior surface to the convex exterior surface of CNTs.^[9-10] This results in a relatively depleted electron density on the interior surface compared to the exterior CNT surface. Thus, the redox properties of metal nanoparticles in contact with either surface could be modified in a different way and the inside iron oxide was easier to reduce than the outside oxide.^[8] The improved reducibility of CNT-confined iron catalyst was found to benefit the formation of iron carbides which are the active phase under Fischer-Tropsch (FT) synthesis conditions and helped improving its catalytic activity.^[11] Similarly, confinement of a bimetallic Rh-Mn catalyst in CNT channels also led to an improved activity for catalyzing syngas conversion to C₂ oxygenates compared to that located on the more accessible exterior surfaces of CNTs.^[12] The enhancement of activities of nanocatalysts confined inside CNTs have also been reported in other reactions.^[13-14] Most recently, Serp and his coworkers observed excellent catalytic performance of PtRu nanoparticles confined inside CNT in selective hydrogenation of cinnamaldehyde.^[15] Although there are likely other effects that could play a role such as the spatial restriction of metal particles, localized concentration of reactants, etc,^[16] we are curious about understanding the effects of the electronic structure of CNTs on the activity of CNT supported catalysts in more detail.

However, it is difficult to probe this small electron density difference between the interior and exterior CNT surface experimentally. Therefore, we turned to ammonia synthesis as a

[a] Ms. S. Guo, Dr. X. Pan, Mr. Z. Yang, Prof. X. Bao
State Key Laboratory of Catalysis, Dalian Institute of Chemical Physics,
Chinese Academy of Sciences
Zhongshan Road 457, Dalian 116023, China
Fax: (+86) 411-84694447
E-mail: panxl@dicp.ac.cn
Baohx@dicp.ac.cn

[b] Ms. H. Gao, Prof. J. Zhao
School of Physics and Optoelectronic Technology and College of
Advanced Science and Technology, Dalian University of Technology
Dalian 116024, China

probe reaction. The ammonia synthesis has been frequently studied as a prototype reaction since it was discovered almost 100 years ago. Based on this reaction, many heterogeneous catalysis concepts have been developed.^[17] It is well accepted that N₂ dissociation is the rate-determining step^[18] and that it is sensitive to the electronic structure of catalysts.^[19] A higher electron density around metal centres facilitates N₂ dissociation because it is an electrophilic process.^[20] The bond of the N₂ molecule is weakened by the incorporation of an electron into its anti-bonding orbital, which was evidenced by an increase in the work function.^[20] This has led to the development of the second generation ammonia synthesis catalysts based on Ru supported on activated carbon (AC) promoted by alkali metals or their oxides e.g. K, where K acts as electron donor.^[21-22] Thus, one can expect that ammonia synthesis over Ru dispersed on the exterior CNT surface will exhibit a higher activity than the inside Ru catalyst, if a shift of electron density from the inner to the outer CNT wall indeed plays a role in the catalytic activity of CNT-supported catalysts. Hence, the effect of confinement in CNTs on the ammonia synthesis activity of Ru catalysts should be opposite to that previously observed for FT synthesis over Fe and C2 oxyneates formation over RhMn catalysts.^[11-12]

Results and Discussion

We prepared two catalysts for comparison in this study. One catalyst has Ru particles dispersed homogeneously inside the CNT channels (denoted as Ru-in-CNT), where the metal loading is 3.5 wt%, as detected by ICP. TEM characterization reveals that the Ru particles are distributed uniformly inside the CNT channels in Ru-in-CNT, as reported in our previous study.^[23] The other catalyst has Ru nanoparticles almost exclusively dispersed on the outside of CNTs (denoted as Ru-out-CNT) and the metal loading is 2.9 wt%. Since activated carbon (AC) has been widely used as support of Ru for NH₃ synthesis, we took a commercial high surface area AC (1040 m² g⁻¹) and carbon black (CB, 80 m² g⁻¹) for comparison.

Figure 1 shows that the turnover frequency (TOF) over Ru-out-CNT is in the range of $1.6\text{-}2.6 \times 10^{-4} \text{ s}^{-1}$ at 400 °C and 20 ml min⁻¹ flow rate in the pressure range of 1- 4 MPa. Interestingly, TOF over Ru-out-CNT is around two times higher than that over the inside Ru catalyst. In comparison, the TOF of the CB supported Ru catalyst (Ru/CB) is almost 5 times lower than that of Ru-in-CNT (Figure 1) while the activity of AC supported Ru (Ru/AC) is negligible. Aika et al. earlier also observed a negligible activity over AC supported Ru catalyst.^[24] For carbon supported Ru catalysts, their surface areas and electron conductivities have frequently been credited for the different activities, which can also explain the difference between Ru/CNT, Ru/CB and Ru/AC here. Although AC has the highest surface area here, it has the worst graphitization degree, which determines its low electron conductivity. In comparison, CB is rather well graphitized but its surface area is 3 times lower than that of nanotubes. CNTs are essentially composed of graphitic layers and thus have the best graphitization degree. Earlier studies demonstrated that Ru catalysts supported on well graphitized carbon or CNT outer surfaces exhibited higher ammonia synthesis activity compared to other carbon materials such as activated carbon.^[22, 25] Song et al. recently studied epitaxially grown Ru particles on a highly oriented pyrolysed graphite (HOPG) surface and found that a well ordered graphitic surface facilitates the dissociation of N₂ on Ru surfaces.^[26]

However, the activity difference between Ru-in-CNT and Ru-out-CNT cannot be simply explained by differences in the electron conductivity and surface area of the CNT support because we have used the same open CNTs for preparation of both catalysts. Furthermore, they have gone through the same reduction procedure prior to reaction tests. An online MS did not detect the release of the electro-negative chlorine from RuCl₃ precursor, which was used in the catalysts preparation, after the reduction procedure (in hydrogen for 12 h at 450 °C) had been completed. Neither were CH₄, CO or CO₂ detected. The BET surface areas of the reduced Ru-in-CNT and Ru-out-CNT were also practically the same ($\sim 280 \text{ m}^2 \text{ g}^{-1}$). It thus can be reasonably assumed that both supports retained similar characteristics even after activation. Therefore, there should be other effects playing roles in the activity difference between Ru-in-CNT and Ru-out-CNT.

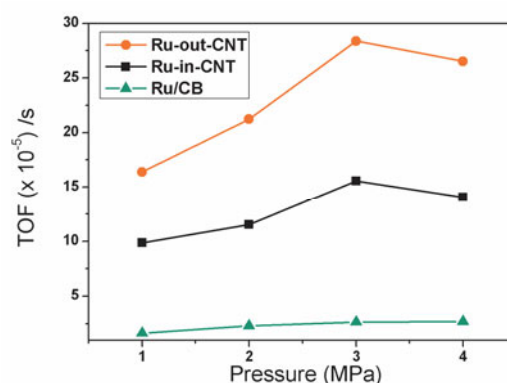


Figure 1. Catalytic activities of Ru-in-CNT and Ru-out-CNT in ammonia synthesis, in comparison to that of Ru/CB. Feed gas composition: 4% Ar/24% N₂/72% H₂ (vol), flow rate: 20 ml min⁻¹, 0.2 g catalyst, reaction temperature: 400 °C.

Figure 2a shows a typical TEM image of the reduced Ru-in-CNT. The particle size is in the range of 2-5 nm (Figure 2c, before reaction), which is smaller than the CNT inner diameter (4-8 nm), leaving sufficient space for transport of reactants and products.^[23] In Ru-out-CNT the particles are also homogeneously dispersed, but on the exterior surface of CNTs (Figure 2b), evidenced by rotating the microscopic specimen. The particle size falls in the same range as that of Ru-in-CNT, but the size distribution is slightly broadened (Figure 2d, before reaction). Further characterization by H₂- and CO-chemisorption confirms that the average particle size of Ru-out-CNT is only slightly larger than that of Ru-in-CNT, as shown in Table 1. Furthermore, one can see from Figures 2c and 2d that even after reaction tests, the particle sizes of both Ru-in-CNT and Ru-out-CNT catalysts do not change significantly, indicating that the catalysts are rather stable under reaction conditions. Thus the particle size difference cannot explain solely the different ammonia synthesis activities over the inside and outside Ru catalysts.

Figure 3 displays the TPR profiles of Ru-in-CNT and Ru-out-CNT along with that of blank CNT. Blank CNT yields two H₂ consumption peaks. One is very weak in the range of 200-300 °C and the other is above 400 °C accompanied by simultaneous release of H₂O (shown as dashed line in Figure 3), but negligible CH₄ emission. Kundu et al. also observed two similar water peaks during TPR of CNTs.^[27] They attributed the very weak peak around 250 °C to the dehydration of neighboring carboxylic groups and the one

above 400 °C with a more than 10 times higher intensity was assigned to the direct reduction of aldehyde, quinone and phenol groups.^[27]

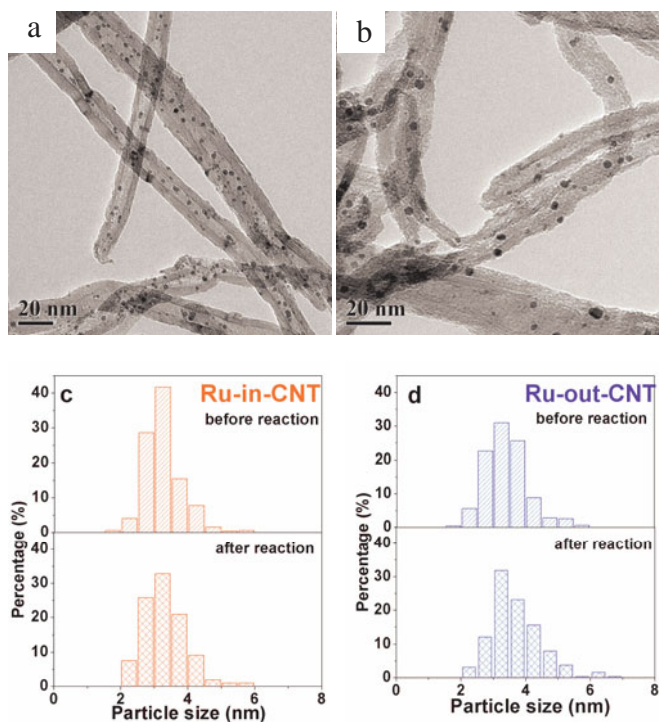


Figure 2. TEM images and the metal particle size distributions of the catalysts after reduction for 12 h at 450 °C in hydrogen: (a) and (c) Ru-in-CNT; (b) and (d) Ru-out-CNT. The particle size distributions after reaction are also included for comparison. They are obtained by measuring 500 particles from randomly taken TEM images over a wide area of the specimen.

Table 1. Metal particle size and dispersion derived from H₂- and CO-chemisorption

Catalyst	Loading	H ₂ -chemisorption		CO-chemisorption	
		Dispersion	Particle size (nm)	Dispersion	Particle size (nm)
Ru-in-CNT	3.5%	23.4%	5.7	29.4%	4.5
Ru-out-CNT	2.9%	21.8%	6.1	24.7%	5.4

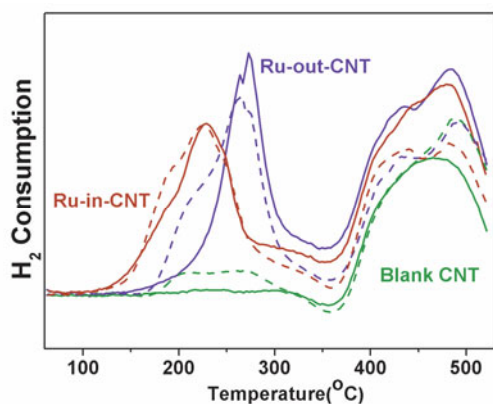


Figure 3. TPR profiles of Ru-in-CNT and Ru-out-CNT in comparison to that of blank CNT. Dashed lines represent the corresponding signals of H₂O detected by mass spectrometer.

Figure 3 shows that another intense H₂ consumption peak appears in the lower temperature range of 200-300 °C over both Ru-in-CNT and Ru-out-CNT catalysts compared to the profile of the blank CNT sample. This peak can be attributed to the reduction of Ru³⁺ to Ru⁰ species. A similar reduction temperature range has been reported for Ru supported on graphitic carbon in an earlier study.^[28] The integrated area of the ruthenium reduction peak of Ru-in-CNT is around 1.2 times that of Ru-out-CNT in Figure 3 which is in accordance with their respective metal loadings. Furthermore, one can see that the reduction of Ru³⁺ takes place around 270 °C for Ru-out-CNT while it occurs at a lower temperature i.e. ca. 230 °C for Ru-in-CNT. This demonstrates that the inside Ru species are easier to reduce compared to the outside ones. This trend of facilitated reduction of oxidic Ru inside CNT channels is consistent with our previous observations for iron oxide.^[7] Since the metal particle size is similar in both catalysts, the facilitated reduction could be due to the interactions between the oxidic ruthenium species and CNT surfaces.

Earlier studies on carbon-supported Ru-based catalysts have revealed the important modification effects of the supports and additives on the local structure of Ru through interactions, in particular the electron density. The work function of single, double and multi-walled CNTs was reported to be in the range of 4.7-4.9 eV.^[29] Upon decoration of Ru nanoparticles, the work function of the composite was lowered due to electron transfer from Ru to the CNT.^[30] Most likely, the outside Ru transfers fewer electrons due to repulsion of electrons since the exterior CNT surface has already a higher electron density. In comparison, it could be easier for the inside Ru to donate more electrons since it is located on the relatively electron deficient interior CNT surface. Therefore, we postulate that the inside and outside Ru catalysts exhibit different electron densities resulting from the Ru-CNT interactions, which can be the reason for the different ammonia synthesis activities over Ru-in-CNT and Ru-out-CNT. We attempted to characterize the electronic state of Ru using XPS. However, it was not successful because it was not possible to obtain sufficient signals from the inside Ru particles due to shielding of the 3-5 nm thick CNT walls.

Therefore, we turned to adsorption microcalorimetry using CO as a probe molecule because this is a widely employed technique, which provides information about the interaction energy of CO with metal surfaces and is sensitive to the electron density of metal centers.^[31] The metal-CO bonding involves electron donation from the CO 5σ orbital to the metal and back-donation from the metal to the CO 2π* orbital. Thus a metal cluster with a higher electron density is expected to result in a stronger metal-CO bonding and consequently should give a higher adsorption heat.

Figure 4 shows the CO adsorption heat as a function of the surface coverage. The initial differential adsorption heat of CO on Ru-in-CNT is 111 kJ mol⁻¹. Note that adsorption of CO was not detectable on blank CNTs. In comparison, Ru-out-CNT exhibits a higher initial adsorption heat (123 kJ mol⁻¹), which implies stronger Ru surface adsorption sites for CO on Ru-out-CNT than on the inside Ru surface. Both initial differential adsorption heat values fall in the range reported earlier for Ru supported on high-surface area graphite with a similar Ru dispersion.^[28] They also agree with the adsorption heat around 125 kJ mol⁻¹ on polycrystalline Ru.^[32] It can be seen that a plateau exists over Ru-in-CNT up to CO coverage of 0.4. It indicates that this catalyst has fairly homogeneous Ru surface sites with regard to their geometry and interaction energies with CO.

Ru-out-CNT has a narrower plateau within the coverage up to 0.2 suggesting less homogeneous Ru surface sites than on the inside Ru. At the coverage higher than 0.5, the adsorption heat over both catalysts decline and the two curves overlap suggesting that the medium and weaker adsorption sites are similar over these two catalysts.

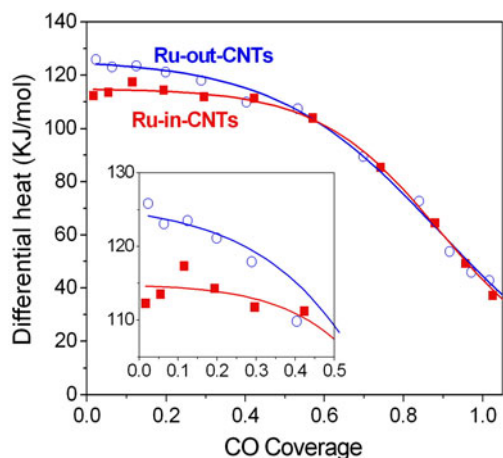


Figure 4. Differential heat of CO adsorption as a function of the surface coverage. The inset shows the adsorption heat in the CO coverage range up to 0.5. The open circles represent Ru-out-CNT while the filled squares denote Ru-in-CNT.

At a very low coverage (close to zero) CO adsorbs in the linear mode.^[33] Therefore, the presence of stronger surface sites for CO adsorption on Ru-out-CNT could be attributed to a higher electron density on the outside Ru centers than the inside ones. This effect is analogous to promoters. For example, Spiewak et al. detected a higher adsorption heat of CO on Ni when it was promoted with K and Cs, which are known to be electron-donating agents.^[31] On the other hand, when carbon supported Ru metal was modified with K, the binding energy of Ru was lowered by 0.1 eV.^[34] Thus, there is an increased density of surface electron states available for back-bonding with $2\pi^*$ orbitals of CO and N_2 . Consequently, the adsorption heat increases, as well as the dissociation probability.^[32] Likewise, relatively higher electron density on the outside Ru should lead to more facile adsorption and activation of N_2 than on the inside Ru catalyst and hence the activity for ammonia synthesis, as we observed in Figure 1.

The postulation of relatively higher electron density on the outside Ru centers is further supported by first principles calculations. Figure 5 shows the differential electron density isosurface of two Ru_6 cluster/ (10, 10) CNT models. It can be seen that the Ru_6 cluster donates electrons to carbon whether it is located inside or outside of the (10, 10) CNT. But the modification of electron density is more pronounced in the case of the inside Ru_6 cluster. Mulliken population analysis indicates that the inside Ru_6 cluster donates 2.41 electrons to the CNT. In comparison, there are only 1.66 electrons transferred from the outside Ru_6 to the CNT. This phenomenon is also observed in other models. For example, in the model consisting of an icosahedral Ru_{13} cluster and a (12, 12) CNT, the inside Ru_{13} cluster donates 0.8 electrons more to the CNT surface than the outside Ru_{13} cluster. When a Ru_6 cluster is placed inside a (8, 8)@(13, 13) double walled CNT, it transfers 1.41 electrons more to carbon than the outside Ru_6 cluster. As a result,

the outside Ru should have a higher electron density than the inside one.

Furthermore, the first principles calculations also show that the CO adsorption heat on atop site of the outside Ru_6 cluster (242 kJ mol^{-1}) is 10 kJ mol^{-1} higher than that on the inside Ru_6 cluster (232 kJ mol^{-1}), which compares well with the experimentally found difference of adsorption heats. The much higher calculated adsorption energies can be attributed to the very small cluster models used in the calculation. On a larger cluster such as a free standing Ru_{13} , the CO adsorption heat decreases to 218 kJ mol^{-1} in comparison to 254 kJ mol^{-1} on a free-standing Ru_6 . For reference, the adsorption heat on Ru (0001) surface was calculated to be 176 kJ mol^{-1} within the same level of theory. It agrees very well with a previously reported value of 174 kJ mol^{-1} obtained from DFT-GGA.^[36] Analysis of the local density of state on the adsorbed CO molecule and the Ru_6 cluster also reveals the coupling between the $2\pi^*$ orbitals of CO with the d orbitals of Ru_6 cluster, whereas this coupling is slightly stronger in the case of outside Ru_6 cluster.

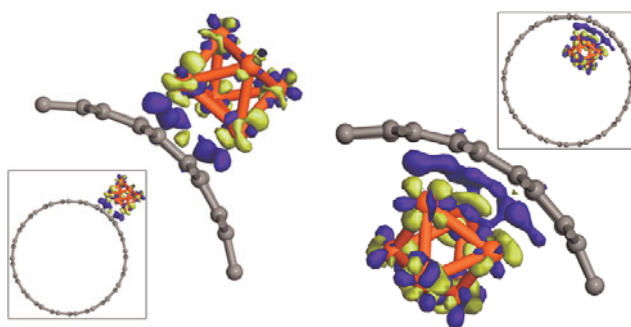


Figure 5. Isosurfaces of the differential electron density (at values of $\pm 0.05 \text{ electrons } \text{\AA}^3$) for Ru_6 -out-CNT (left) and Ru_6 -in-CNT (right). The inserts show the full cross section pictures of the isosurfaces. The grey balls represent the carbon atoms of the (10, 10) CNT. Red bars denote the Ru-Ru bonds. The blue areas suggest enriched electron density and the yellow areas depleted density with respect to free-standing clusters.

Conclusion

In summary, TPR, CO adsorption microcalometry, and first principles calculations suggest that the Ru located on the exterior CNT surface has a higher electron density than the inside Ru due to the Ru-CNT interactions although both catalysts have very similar metal particle sizes and dispersion according to TEM, CO and H_2 chemisorption analysis. This is consistent with the electron density difference between the exterior and interior CNT surface due to graphene curvature.^[10, 11] Since the adsorption and dissociation of N_2 is an electrophilic process, the outside Ru catalyst consequently is more conducive to N_2 activation and hence its activity for ammonia synthesis is higher than that of the inside Ru catalyst. This study leads further support to the concept that electron transfer from the curved graphene walls of CNTs could play an important role for the activity of catalysts confined on inside and outside CNT surfaces. It provides a novel approach to modulate activities of metal catalysts which holds great promise but has been hardly explored yet. We anticipate that further theoretical and experimental studies will lead to developments of novel functional nanomaterials and nanotechnologies based on nanotubes for electronics, magnetic storage, or sensor applications.

Experimental Section

Catalyst Preparation: CNTs have been purchased from Chengdu Organic Chemicals (MFG code M12020702R). The inner and outer diameters were 4-8 and 10-20 nm, respectively. CNTs were pre-treated in concentrated HNO₃ (68 wt %) at 130 °C for 12 h, which led to opened and shortened nanotubes. Ru-in-CNT was prepared following a previously reported method. Briefly, acetone was used as a solvent for RuCl₃ because of its low surface tension, which can facilitate the introduction of metal salt solution into CNT channels by a wet chemistry method. Ultrasonic treatment and extended stirring were employed to aid the capillary forces of CNTs in order to obtain a homogeneous dispersion of Ru nanoparticles. Subsequent slow drying at 110 °C in air resulted in most Ru particles (over 80%) being introduced into CNT channels. For preparation of Ru-out-CNT, we used open CNTs of exactly the same batch and the same treatment as for the Ru-in-CNT catalyst. Therefore, xylene was used to temporarily block the CNT channels before decoration of the exterior CNT surface with RuCl₃.^[23] Water was chosen as a solvent for RuCl₃ because it is immiscible with xylene, which can prevent RuCl₃ solution from infiltrating the channels. Furthermore, in comparison to water the higher boiling point of xylene allows preferential evaporation of water on the outside of nanotubes. Thus only the external surfaces were decorated with ruthenium. After evaporation of xylene at 80 °C, the same drying procedure was applied to Ru-out-CNT.

Carbon black (CB) was purchased from Alfa Aesar and activated carbon (AC) from Beijing Guanghua Woods Ltd.. Ru/CB and Ru/AC were prepared following the same procedure as that of Ru-in-CNT.

Catalyst Characterization: Catalysts were usually pre-reduced before characterization and reaction tests in hydrogen for 12 h at 450 °C unless otherwise stated. Specific BET surface areas were measured by N₂ adsorption on an ASAP 2020 apparatus. TEM measurements were carried on a FEI Tecnai G² microscope operated at an accelerating voltage of 120 kV. H₂ chemisorption and CO adsorption microcalorimetry were carried out at 40 °C on a Quantachrome Autosorb-1/C Chemisorb apparatus and a Setaram heat flow microcalorimeter (BT2.15 heat-flux calorimeter), respectively. Prior to measurements, the pre-reduced catalysts were further reduced in situ for 2 h at 450 °C in H₂. Detailed description of the setup and procedure of microcalorimetric measurements can be found in an earlier study.^[31] The metal dispersion and particle size were also estimated based on assumption of a spherical geometry of the particles and an adsorption stoichiometry of one hydrogen atom and one CO molecule on one Ru surface atom. The particle size was estimated according to the equation:

$$d = 6 \frac{V_M}{S_M * D_M} = \frac{M * 6 * \rho_{site}}{\rho_{metal} * N}$$

where V_M the volume/atom in the bulk, S_M the average surface area occupied by a metal atom, D_M the dispersion, M the molecular weight, ρ_{site} the Ru surface site density and N the Avogadro number. Thus, d can be calculated according to 1.33/D_M (nm).^[37]

TPR experiments were carried out on a home-built four channel reactors equipped with an online 6-channel mass spectrometer (Omnistar GSD 301 O₂ & GSS 300) as the detector. Prior to reduction, the samples were treated in situ in a He flow (20 ml min⁻¹) for 90 min at 110 °C. Then they were heated from 50 °C to 550 °C at a rate of 2 °C min⁻¹ in 3% H₂/Ar (V/V) (10 ml min⁻¹). Simultaneously, signals of m/e = 2, 15 and 18 (corresponding to H₂, CH₄ and H₂O, respectively) were monitored.

Catalytic Reaction: Ammonia synthesis was carried out on the same four-channel reactors. The pre-reduced catalysts were further activated in H₂ for 2 h at stepwise increasing temperatures 300, 350, 400 and 450 °C, and finally held for 6 h at 475 °C before being cooled to the reaction temperature (400 °C). A stoichiometric mixture of N₂:H₂ = 1:3 (vol) was used as feed gas, which was further dehydrated and deoxygenated before passing to the catalyst beds. The effluent of each channel was absorbed individually by H₂SO₄ aqueous solution containing methyl red as an indicator. The TOF was calculated based on H₂ chemisorption data. Note that the purity of all gases was 99.999%.

Computational Methods: In first principles calculations, we used an infinite (10, 10) single-walled CNT with one-dimensional periodic boundary condition applied along the tube axis. The simulation supercell included four CNT unit cells (160 carbon atoms in total) with one octahedral Ru₆ cluster located either inside or outside of the tube. Other sized Ru clusters such as icosahedral Ru₁₃ and double-walled CNTs were also considered. The CASTEP program was used,^[38] which was based on density function theory (DFT), ultrasoft pseudopotentials and plane-wave basis sets with a cutoff energy of 400 eV. The exchange-correlation interaction was described by the generalized gradient approximation (GGA) with PW91 parameterization.^[39]

Acknowledgements

We thank Mr. Lin Li for helping on the microcalorimetry experiments and Prof. Jianyi Shen from Nanjing University for fruitful discussion on the microcalorimetry results. The authors acknowledge the financial support from the National Natural Science Foundation of China (20503033), the Ministry of Science and Technology of China

(2006CB932703) and the Program for New Century Excellent Talents in University of China (NCET06-0281).

- [1] S. C. Tsang, Y. K. Chen, P. J. F. Harris, M. L. H. Green, *Nature* **1994**, 372, 159-162.
- [2] A. N. Khlobystov, D. A. Britz, G. A. D. Briggs, *Acc. Chem. Res.* **2005**, 38, 901-909.
- [3] J. Sloan, A. I. Kirkland, J. L. Hutchison, M. L. H. Green, *Acc. Chem. Res.* **2002**, 35, 1054-1062.
- [4] H. Friedrich, P. E. de Jongh, A. J. Verkleij, K. P. de Jong, *Chem. Rev.* **2009**, 109, 1613-1629.
- [5] M. D. Halls, H. B. Schlegel, *J. Phys. Chem. B* **2002**, 106, 1921-1925.
- [6] P. Kondratyuk, J. T. Y. Jr., *Acc. Chem. Res.* **2007**, 40, 995-1004.
- [7] W. Chen, X. Pan, M.-G. Willinger, D. S. Su, X. Bao, *J. Am. Chem. Soc.* **2006**, 128, 3136-3137.
- [8] W. Chen, X. Pan, X. Bao, *J. Am. Chem. Soc.* **2007**, 129, 7421-7426.
- [9] R. C. Haddon, *Science* **1993**, 261, 1545-1550.
- [10] D. Ugarte, A. Chatelain, W. A. d. Heer, *Science* **1996**, 274, 1897-1899.
- [11] W. Chen, Z. Fan, X. Pan, X. Bao, *J. Am. Chem. Soc.* **2008**, 130, 9414-9419.
- [12] X. Pan, Z. Fan, W. Chen, Y. Ding, H. Luo, X. Bao, *Nature Mater.* **2007**, 6, 507-511.
- [13] Y. Zhang, H.-B. Zhang, G.-D. Lin, P. Chen, Y.-Z. Yuan, K. R. Tsai, *Appl. Catal. A: General* **1999**, 187, 213-224.
- [14] A. M. Zhang, J. L. Dong, Q. H. Xu, H. K. Rhee, X. L. Li, *Catal. Today* **2004**, 93, 347-352.
- [15] E. Castillejos, P.-J. Debouttière, L. Roiban, A. Solhy, V. Martinez, Y. Kihn, O. Ersen, K. Philippot, B. Chaudret, P. Serp, *Angew. Chem. Int. Ed.* **2009**, 48, 2529-2533.
- [16] X. Pan, X. Bao, *Chem. Commun.* **2008**, 6271-6281.
- [17] G. Ertl, *Angew. Chem. Int. Ed.* **2008**, 47, 3524-3535.
- [18] O. Hinrichsen, *Catal. Today* **1999**, 53, 177-188.
- [19] C. J. H. Jacobsen, S. Dahl, P. L. Hansen, E. Törnqvist, L. Jensen, H. Topsøe, D. V. Prip, P. B. Møenshaug, I. Chorkendorff, *J. Mol. Catal. A: Chemical* **2000**, 163, 19-26.
- [20] K. I. Aika, H. Hori, A. Ozaki, *J. Catal.* **1972**, 27, 424-431.
- [21] H. B. Chen, J. D. Lin, Y. Cai, X. Y. Wang, J. Yi, J. Wang, G. Wei, Y. Z. Lin, D. w. Liao, *Appl. Surf. Sci.* **2001**, 180, 328-335.
- [22] C. Liang, Z. Wei, Q. Xin, C. Li, *Appl. Catal. A: General* **2001**, 208, 193-201.
- [23] C. Wang, S. Guo, X. Pan, W. Chen, X. Bao, *J. Mater. Chem.* **2008**, 18, 5782-5786.
- [24] K. Aika, A. Ohya, A. Ozaki, Y. Inoue, I. Yasumori, *J. Catal.* **1985**, 92, 305-311.
- [25] ZbigniewKowalczyk, J. S. a. S. a. Jodzis, E. zbietaMizera, J. oralski, T. Paryjczak, RyszardDiduszko, *Catal. Lett.* **1997**, 45, 65-72.
- [26] Z. Song, T. Cai, J. C. Hanson, J. A. Rodriguez, J. Hrbek, *J. Am. Chem. Soc.* **2004**, 126, 8576-8584.
- [27] S. Kundu, Y. Wang, W. Xia, M. Muhler, *J. Phys. Chem. C* **2008**, 112, 16869-16878.
- [28] A. Guerrero-Ruiz, P. Badenes, I. R. Águez-Ramos, *Appl. Catal. A: General* **1998**, 173, 313-321.
- [29] P. Liu, Q. Sun, F. Zhu, K. Liu, K. Jiang, L. Liu, Q. Li, S. Fan, *Nano Lett.* **2008**, 8, 647-651.
- [30] C. Liu, K. S. Kim, J. Baek, Y. Cho, S. Han, S.-W. Kim, N.-K. Min, Y. Choi, J.-U. Kim, C. J. Lee, *Carbon* **2009**, 47, 1158-1164.
- [31] B. E. Spiewak, J. Shen, J. A. Dumesic, *J. Phys. Chem.* **1995**, 99, 17640-17644.
- [32] G. A. Somorjai, Wiley, New York, **1994**, pp. 301-313.
- [33] H. Pfiir, D. Menzel, F. M. Hoffmann, A. Ortega, A. M. Bradshaw, *Surf. Sci.* **1980**, 93, 431-452.

-
- [34] I. Rossetti, N. Pernicone, L. Forni, Appl. Catal. A: General **2001**, 173, 271-278.
- [35] G. Ertl, M. Weiss, S. B. Lee, Chem. Phys. Lett. **1979**, 60, 391-394.
- [36] B. Hammer, Y. Morikawa, K. Nørskov, Phys. Rev. Lett. **1996**, 76, 2141-2144.
- [37] J. J. F. Scholten, A. P. Pijpers, A. M. L. Hustings, Cat. Rev. - Sci. Eng. **1985**, 27, 151-206.
- [38] S. J. Clark, M. D. Segall, C. J. Pickard, P. J. Hasnip, M. I. J. Probert, K. Refson, M. C. Payne, Z. Kristallogr. **2005**, 220, 567-570.
- [39] J. P. Perdew, J. A. Chevary, S. H. Vosko, K. A. Jackson, M. R. Pederson, D. J. Singh, Phys. Rev. B **1992**, 46, 6671-6687.
-

Received: ((will be filled in by the editorial staff))
Revised: ((will be filled in by the editorial staff))
Published online: ((will be filled in by the editorial staff))

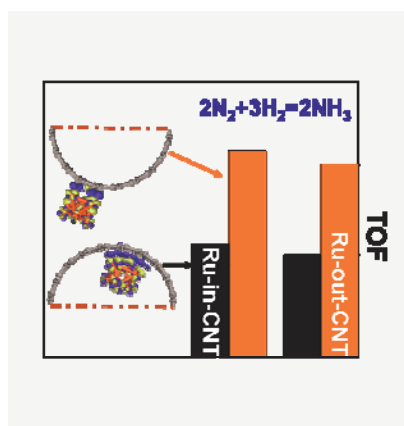
Entry for the Table of Contents (Please choose one layout only)

Layout 1:

Chemistry in carbon nanotubes

Shujing Guo, Xiulian Pan, Haili Gao, Zhiqiang Yang, Jijun Zhao, Xinhe Bao** Page – Page

Probing the electronic effect of carbon nanotube in catalysis: NH₃ synthesis over Ru nanoparticles



NH₃ synthesis over Ru was studied as a probe reaction. The results show that the electronic structure of metal nanoparticles on carbon nanotube surfaces is modified. The inside Ru exhibits a relatively lower electron density due to the Ru-CNT interaction and hence leads to a lower NH₃ synthesis activity than the outside Ru.